Tunable dual-wavelength filter and its group delay dispersion in domain-engineered lithium niobate

Guang-hao Shao, Jing Song, Ya-ping Ruan, Guo-xin Cui,[a] and Yan-qing Lu[b]
National Laboratory of Solid State Microstructures, College of Engineering and Applied Sciences, Nanjing University, Nanjing 210093, China

(Received 12 August 2016; accepted 4 December 2016; published online 16 December 2016)

A tunable dual-wavelength filter is experimentally demonstrated in domain-engineered lithium niobate. Application of an electric field on the y-surfaces of the sample results in the optical axes rotating clockwise and anticlockwise, which makes selective polarization rotation. The quasi phase-matching wavelengths could be adjusted through suitable domain design. A unique dual valley spectrum is obtained in a periodically poled lithium niobate structure with a central defect if the sample is placed between two parallel polarizers. The expected bandwidth could be varied from ~1 nm to ~40 nm. Moreover, both the spectral response and group delay dispersion could be engineered. [http://dx.doi.org/10.1063/1.4972281]

I. INTRODUCTION

Lithium niobate (LN) has been widely studied for more than three decades. It is considered to be "the silicon of photonics" for its versatile nonlinear optical, electro-optic (EO), acousto-optic, and piezoelectric properties.[1,2] Besides, with the state-of-the-art poling and micro-fabrication techniques, complex domain structures can be fabricated precisely,[3] which makes domain engineering of LN a convenient platform to demonstrate new physical mechanisms and develop fascinating applications. Nonlinear frequency conversion, polarization rotation, and macro-phonon polariton excitation have been previously demonstrated in periodically poled LN (PPLN).[4–7] Additionally, the combination of EO and nonlinear effects was utilized to predict polarization insensitive optical parametric amplification in a four section PPLN,[8] which may have promising engineering applications.

On the other hand, dual-wavelength operation is desirable for coherent pulse synthesis, THz generation, and pump-probe experiments.[9–11] A variety of studies have reported on the realization of dual-wavelength lasers based on different materials, such as erbium-doped fibers, semiconductor optical amplifiers, and polarization maintaining fibers.[12–14] To obtain dual-wavelength or multi-wavelength filters, two Peltier devices were used to control the sample's temperature at different positions independently.[15] Simulated annealing (SA) method were employed to realize multi-wavelength operation.[16,17] However, the corresponding domain structures are difficult to fabricate for current poling technique. In addition, normally there are unwanted sidebands in the transmission spectrum. Therefore, it would be desired to design and develop tunable dual-wavelength filters with simple structure and clean transmission spectrum.

In this work, we experimental demonstrated a tunable dual-wavelength filter based on PPLN with a central defect. Light propagates along the x-axis while external DC electric fields are applied on the y-surface of the sample. The sample is placed between two parallel polarizers. In this condition, light satisfying the EO quasi-phase matching (QPM) condition maintains its original polarization state while undergoing polarization rotation and then reverting to the original polarization state.

[a] cuiguoxin@nju.edu.cn
[b] yqlu@nju.edu.cn

In addition, wavelengths far from the QPM point could pass through the sample freely. However, light with wavelengths near the QPM point will change its polarization state, resulting in two transmission minima, and the depth of the minima can be tuned by changing the external electric fields. A tunable dual-wavelength filter is thus obtained in the telecomm band. The bandwidth of the two minima could be tailored with different defect thickness and sample length. Moreover, the group delay dispersion (GDD) around these wavelengths could be tuned effectively.

II. TUNABLE DUAL-WAVELENGTH FILTER BASED ON A PPLN WITH A CENTRAL DEFECT

Figure 1 shows the schematic diagram of our proposed PPLN with a defect in the center of the sample. Light propagates along the x-axis while an external electric field is applied on the y-surface. Owing to the EO effect, the x-axis remains constant while the other two axes rotate a small angle θ about the x-axis:

$$\theta \approx \frac{\gamma_{51} E}{\left(1/n_e^2\right) - \left(1/n_o^2\right)}, \tag{1}$$

where E, γ_{51}, n_e, n_o are the external electric field, EO coefficient, and refractive indices of the extraordinary wave and ordinary wave, respectively. The sign of the EO coefficient changes along with the spontaneous polarization direction, which means that the EO coefficient is also periodically modulated. Thus, the azimuthal angle of the new y-axis changes from $+\theta$ to $-\theta$ successively. The domain thickness should satisfy the QPM condition for the EO effect at a certain wavelength.[2] In this case, the reciprocal vector provided by the sample could compensate the phase mismatch between ordinary and extraordinary waves. In another words, each domain serves as a narrow-band half wave plate with varying fast axes. Though LN has strong nonlinear optical effects, they are not considered here for several reasons. First, the reciprocal vector designed in our proposal does not satisfy the nonlinear QPM condition.[1] Besides, the intensity of the injected wave is weak, and thus the efficiency of the nonlinear process is quite low. The thickness of the central defect is doubled in comparison with other domains. In this case, our sample could be treated as two mirrored samples with N periods bonding together. The original resonance peak is thus split into two symmetrical ones in a similar manner to an artificial optical dimer.

Jones matrix calculus is used here to describe the process.[18] The polarization state of the output wave is determined by that of the input wave E_{in} and the transformation matrix of the entire sample T, such that $E_{out} = T \bullet E_{in}$, and

$$T = \prod_{n=1}^{2N} R(\theta_n) W_n R(-\theta_n), \tag{2}$$

where the rotation matrix $R(\theta_n)$ and the intrinsic Jones Matrix of the n^{th} domain W_n can be expressed as

$$R(\theta_n) = \begin{pmatrix} \cos\theta_n & \sin\theta_n \\ -\sin\theta_n & \cos\theta_n \end{pmatrix}, \tag{3}$$

$$\text{and} \quad W_n = \begin{pmatrix} e^{-in_o\omega l_n/c} & 0 \\ 0 & e^{-in_e\omega l_n/c} \end{pmatrix}. \tag{4}$$

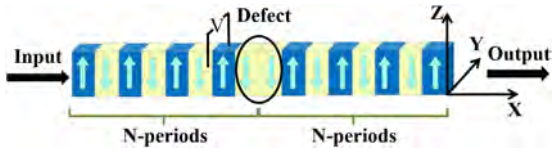

FIG. 1. Schematic diagram of a PPLN sample with a central defect.

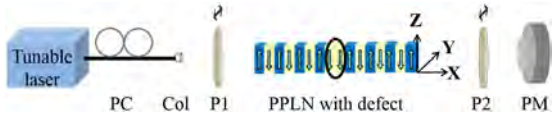

FIG. 2. Schematic diagram of the experimental setup for analyzing the transmission spectrum. The sample is placed between two parallel polarizers. PC, polarization controller; Col, collimator; P1 and P2, polarizers; PM, power meter.

In Eqs. (3) and (4), θ_n is the corresponding azimuthal angle with opposite signs in different domains, that can be deduced from Eq. (1), ω is the angular frequency, c is the speed of light in a vacuum, and l_n is the thickness of the n^{th}-domain. The duty cycle of the sample is set as 50%. In this case, the defect thickness is doubled. Without loss of generality, we assume that the injected wave is y-polarized (ordinary wave) in this work. The sample produces $4N\theta$ polarization rotation in the first N-periods owing to the EO effect. Because the structure is axially symmetric, a $-4N\theta$ total rotation will take place in the second N-periods, and thus the final polarization state would fully recover as the ordinary wave at the wavelength satisfying the QPM condition.

The thickness of one period was set at 20.48 μm. And the temperature was maintained at 40 °C. According to the QPM condition, the matching wavelength should be 1585 nm. Figure 2 shows the schematic diagram of our experimental setup. The sample with 500 periods (N = 250) was placed between two y-direction parallel polarizers. A tunable laser and a power meter were used to measure the spectrum and output power. Figure 3(a) shows the simulation result. We can see that light at wavelengths exactly at, and far from, the QPM condition maintain their original polarizations after exiting the sample. However, adjacent wavelengths close to the QPM point exhibit EO-tunable polarizations with two minima in the transmission spectrum. Moreover, with the increase of the electric fields, the minima become deeper with larger contrast. Consequently, the transmission spectrum exhibits a dual-wavelength filtering characteristic, which could be further tuned by changing the applied electric field.

The selected sample (HC Photonics Corp.) contains 500 periods and the interaction length is 10.24 mm, with the dimension of 1 mm and 0.5 mm in y and z direction, respectively. Chromium (Cr) electrodes were coated on the y-surfaces. Stainless steel probes contacted the electrodes and were connected to a high voltage supplier (Stanford Reserch Systems, Inc. Modal PS350). A tunable laser (Agilent 9140A) was used to scan wavelengths from 1578 nm to 1592 nm in steps of 0.1 nm. In order to record the EO tuning process, the electric fields of 0 to 900 V/mm were applied in steps of 100 V/mm. Figure 3(b) shows our experimental results. The QPM wavelength is 1585.3 nm, which is close to the theoretical prediction. As LN is very sensitive to temperature, the transmission spectrum varied by several hundred picometers during the measurement, owing to the stability of our temperature controller (HC Photonics Corp.) being limited to ± 0.1 °C. The actual electric fields are higher than theoretical ones, which still don't have an concrete explanation. Furthermore, we find that

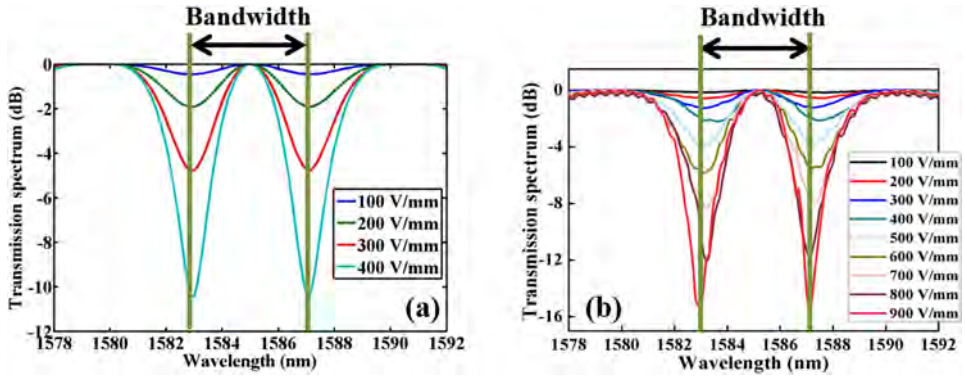

FIG. 3. Theoretical (a) and experimental (b) results of the transmission spectrum. The bandwidth is the wavelength difference between the two valleys.

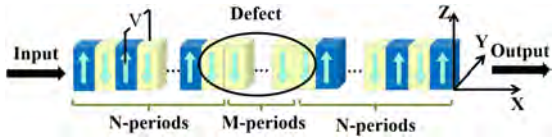

FIG. 4. Schematic diagram of a more general case for a tunable dual-wavelength filter.

the deepest minima appear when the electric field is around 900 V/mm, with a contrast of -15.6 dB, which means that the transmission intensity reduces to ~ 2% of its origin at the wavelength of the minima of the two valleys. Furthermore, the largest contrast ratio of each electric field fits a cosine function, which matches the simulation results according to Jones matrix calculus.

Figure 4 shows a schematic diagram of a more general case for the dual wavelength filter. The bandwidth between two minima could be tailored by modifying the parameters M and N. Similarly to the case shown in Fig. 1, the last domain in the first part and the first domain in the last part also belong to the defect. Therefore, in our previous case, M equals zero and N equals 250. As mentioned before, each domain acts like a half wave plate with varying fast axes at the QPM wavelength. In this case, light satisfying the QPM condition is always linearly polarized at the end of each domain. Besides, the phase matching light will recover to its original polarization state only if the structure is symmetrical. In other words, if the parameters (M and N) are not integers or the sample is asymmetrical, then the polarization state evolution and corresponding transmission become more complicated, and the dual-minima spectrum disappears.

For a practical and applicable analysis, we assume the sample length is longer than 1 mm and shorter than 40 mm. Giving the PPLN period of 20.48 μm as an example, $2N + M$ should be larger than 50 and less than 2000. Moreover, the bandwidth mainly depends on the structure itself. As for our design described in Fig. 3 ($M = 0$ and $N = 250$), we can see that the bandwidth has no apparent change in both theoretical simulation and experimental demonstrations. In order to perform a more precise analysis, assuming the electric field varies from 0 to 500 V/mm, the bandwidth only theoretically changes by 0.2 nm, as shown in Fig. 5(a).

Here, we set M equals to zero so that $25 \leq N \leq 1000$, and study the relationship between N, M and bandwidth. When an electric field of 100 V/mm is applied, the bandwidth becomes narrower with larger N, which means a longer sample, as shown in Fig. 5(b). It could vary from 40.01 nm to 1.03 nm. From our simulation, the bandwidth is inversely-proportional to N, *i.e.*, bandwidth is ~1057 nm/N. As for the defect thickness, if M varies from 0 to 100 under the condition of N =250 and E = 100 V/m,

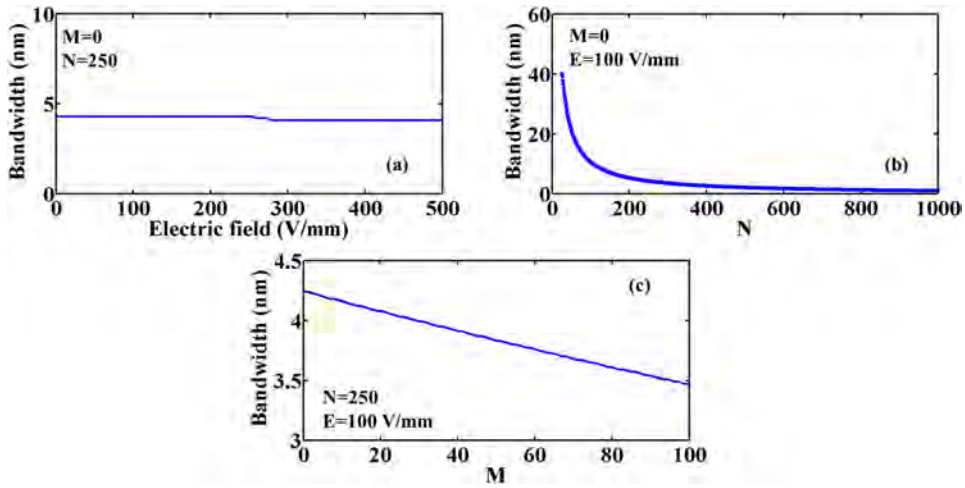

FIG. 5. Analysis of the relationship between bandwidth, electric field, N and M. (a) Bandwidth dependence on electric field assuming M = 0 and N = 250. (b) Bandwidth versus N for M = 0 and E = 100 V/mm. (c) Bandwidth versus M for N = 250 and E = 100 V/mm.

the bandwidth changes from 4.24 nm to 3.47 nm. It shows that N plays a more important role in bandwidth than M. Moreover, the QPM wavelength mainly depends on the thickness of a domain. The transparent window of LN is 400 nm to 4000 nm; thus, the corresponding domain thickness should be 4.3 μm to 86.5 μm, which can be easily fabricated. Similar designs could therefore operate at any wavelength from 400 to 4000 nm.

III. GROUP DELAY DISPERSION CHARACTERISTICS

The GDD is also an important feature of various optical components. Thus, it is important to investigate the GDD for different electric fields and M. The group delay (GD) can be obtained from the first order derivative of $\varphi(\omega)$ (the relative phase delay) to the frequency, while the GDD is the first order derivative of the GD to the frequency in the same way, as shown in Eqs. (5) and (6).[19]

$$GD = -\frac{d\varphi(\omega)}{d\omega} \tag{5}$$

$$GDD = \frac{d^2\varphi(\omega)}{d\omega^2} \tag{6}$$

At the QPM wavelength, the y-polarized injected wave rotated to extraordinary direction and then changed back to the ordinary wave. As LN is a uniaxial negative crystal, the group velocity of the ordinary wave is smaller than the extraordinary wave. It results in the GD at QPM point lower than any other wavelength. The symmetrical structure leads to the GD spectrum also being symmetric, which means that the first order derivative of GD at the QPM point is zero. In other words, the GDD at the wavelength satisfying QPM is always zero.

We take $M = 0$ and $N = 250$ as an example to analyze the relationship between GDD and electric field, as shown in Fig. 6(a). The resonance becomes stronger with higher electric field. Therefore, the peak of GDD in the spectrum becomes larger. Previously, M was maintained at zero, and thus it is of interest to understand the dependence of GDD and the slope at QPM point on M. In this condition, the defect acts as a phase retarder. If we assume M varies from 0 to 100, which means that the defect is in the range of 40 μm to 2 mm, then with 300 V/mm and N equal to 250, the dispersion peak could vary from 1.41 ps^2 to 3.86 ps^2. Moreover, the slope at the matching wavelength could be changed from 0.6457 ps^2/nm to 1.1354 ps^2/nm, as shown in Figs. 6(b) and (c), respectively.

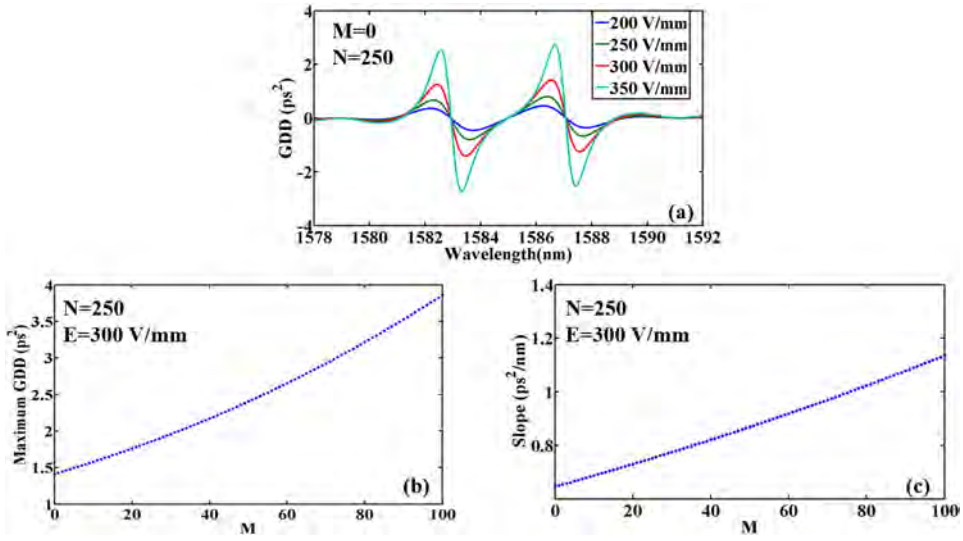

FIG. 6. Analysis of the relationship between GDD, electric field, M, and the slope at the QPM point. (a) The dispersion spectrum under different electric fields, with $M = 0$ and $N = 250$. (b) Maximum GDD in the spectrum versus M, with $N = 250$ and $E = 300$ V/mm. (c) The slope at the QPM point versus M, with $N = 250$ and $E = 300$ V/mm.

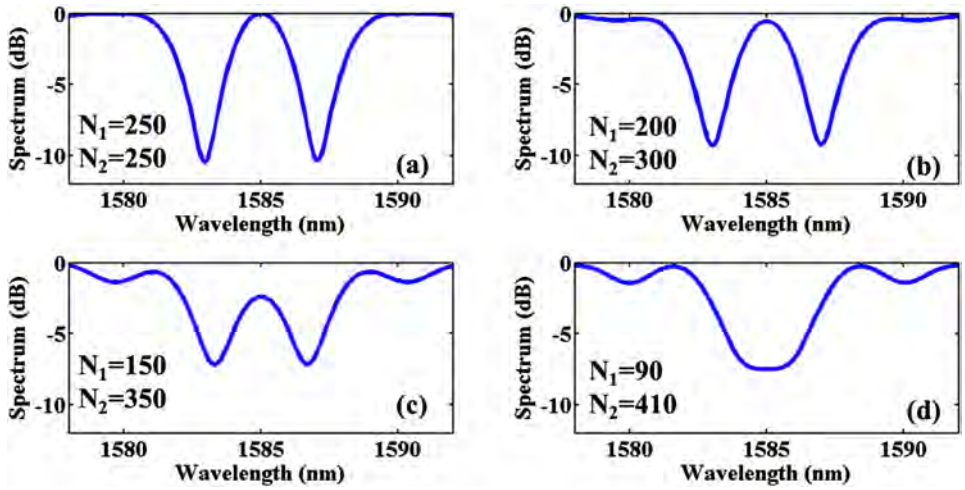

FIG. 7. Transmission spectrum of different structures under the condition of E = 400 V/m and M = 0. (a) N_1 = 250, N_2 = 250, (b) N_1 = 200, N_2 = 300, (c) N_1 = 150, N_2 = 350, and (d) N_1 = 90, N_2 = 410.

IV. DISCUSSION

In this study, we investigated the polarization evolution in a domain engineered LN, and proposed an approach to obtain a tunable dual-wavelength filter. A pair of parallel polarizers were utilized in order that the wavelength-dependent polarization change was converted to a transmission curve with two depth-tunable minima. However, if two cross polarizers were employed, a reciprocal dual-peak spectrum could be achieved. This feature has potential for interesting applications in dual-wavelength laser systems. The filtering or lasering wavelength could be tuned by the applied electric field, temperature. Furthermore, an asymmetrical PPLN structure, which means that the defect is not in the center, could be used to obtain a transmission curve with different contrast ratio between minima and QPM wavelength. Figure 7 shows the transmission spectrum of different structures at E = 400 V/m and M = 0, where N_1 and N_2 are the periods of first and second parts, respectively. For different parameters, different contrast ratios are exhibited, such as 10.45 dB, 8.77 dB, 4.807 dB. Even 0 dB contrast are achieved for N_1 = 90 and N_2 = 410, where a flat bottom spectrum comes out.

On the other hand, dispersion control is also an important parameter in many optical devices. We have predicted that the dispersion could be modulated by electric field, wavelength, and the domain structure of our sample. Among them, the electric field and wavelength are more practical and convenient parameters for tailoring the dispersion. Taking M = 0 and N = 250 as an example, the dispersion changes along with different wavelengths and different electric field are obtained as shown in Fig. 6(a). It is interesting to see that the dispersion could be switched from positive to negative by modifying the direction of the electric field. Although the dispersion tuning range is not very wide, we believe it may be enhanced by employing an cavity. The use of high reflection coatings at both end-surfaces would lead to light travelling many times back and forth, with a consequently much longer interaction length, meaning that the dispersion tuning could be more effective. This could potentially find some interesting applications in EO phase shifters.

In this work, only the EO effect is considered. However, as we mentioned earlier, domain-engineered LN is also a well-acknowledged platform for linear, nonlinear, and polariton interactions.[20,21] If the findings in our work could be compatible and coupled with some other physical processes through suitable domain design, then more exiting physical phenomena and applications would be expected.

V. CONCLUSIONS

In conclusion, we have proposed a design for a tunable dual-wavelength filter based on PPLN with a defect. The EO effect is introduced by applying external electric fields along the y-axis.

The injected y-polarized wave at the QPM point converts to a z-polarized wave and then reverts to the original polarization state. Therefore, the output wave still maintains its original polarization owing to the symmetrical design. If the sample is placed between two y-direction parallel analyzers, the spectrum exhibits a pair of narrow transparency minima. The depth of the minima could be tuned by applying different electric field. The state-of-the-art domain engineering technique allows control of the bandwidth and central wavelength of the spectrum. Besides, the GDD of our structure could be effectively modulated by the electric field, wavelength, and the domain structure of our sample.

ACKNOWLEDGMENTS

Guang-hao Shao thanks Dr. Chao Zhang for his fruitful discussion. This work was supported by National Natural Science Foundation of China (Grants No. 61490714 and No. 11604144).

[1] M. M. Fejer, G. A. Margel, D. H. Jundt, and R. L. Byer, J. Quantum Electron. **28**, 2631 (1992).
[2] Y. Q. Lu, Z. L. Wan, Q. Wang, Y. X. Xi, and N. B. Ming, Appl. Phys. Lett. **77**, 3719 (2000).
[3] V. Ya. Shur, A. R. Akhmatkhanov, and I. S. Baturin, Appl. Phys. Rev. **2**, 040604 (2015).
[4] Y. Sheng, D. Ma, M. Ren, W. Chai, Z. Li, K. Koynov, and W. Krolikowski, Appl. Phys. Lett. **99**, 031108 (2011).
[5] X. F. Chen, J. H. Shi, Y. P. Chen, Y. M. Zhu, Y. X. Xia, and Y. L. Chen, Opt. Lett. **28**, 2115 (2003).
[6] N. V. Bloch, K. Shemer, A. Shapira, R. Shiloh, I. Juwiler, and A. Arie, Phys. Rev. Lett. **108**, 233902 (2012).
[7] X. S. Song, F. Xu, and Y. Q. Lu, Opt. Lett. **36**, 4434 (2011).
[8] G. H. Shao, X. S. Song, F. Xu, and Y. Q. Lu, Opt. Express **20**, 19343 (2012).
[9] L. S. Ma, R. K. Shelton, H. C. Kapteyu, M. M. Murnane, and J. Ye, Phys. Rev. A **64**, 021802 (2001).
[10] K. Kawase, T. Hatanaka, H. Takahashi, K. Nakamura, T. Taniuchi, and H. Ito, Opt. Lett. **25**, 1714 (2000).
[11] A. Yu, X. Ye, D. Ionascu, W. Cao, and P. M. Champion, Rev. Sci. Instrum. **76**, 114301 (2005).
[12] G. E. Town, L. Chen, and P. W. E. Smith, IEEE Photonics Technol. Lett. **12**, 1459 (2000).
[13] H. Dong, G. Zhu, Q. Wang, H. Sun, and N. Dutta, Opt. Express **12**, 4297 (2004).
[14] Y. D. Gong, X. L. Tian, M. Tang, P. Shum, M. Y. W. Chia, V. Paulose, J. Wu, and K. Xu, Opt. Commun. **265**, 628 (2006).
[15] J. H. Wang, J. H. Shi, Z. E. Zhou, and X. F. Chen, Opt. Express **15**, 1561 (2007).
[16] C. H. Lin, Y. H. Chen, S. W. Lin, C. L. Chang, Y. C. Huang, and J. Y. Chang, Opt. Express **15**, 9859 (2007).
[17] C. L. Chang, Y. H. Chen, C. H. Lin, and J. Y. Chang, Opt. Express **16**, 18535 (2008).
[18] A. Yariv, and P. Yeh, *Optical waves in crystal* (John Wiley & Sons, New York, 1984) p. 121.
[19] A. Yariv and P. Yeh, *Photonics: Optical electronics in modern communications* (Oxford University Press, New York, 2007), p. 15.
[20] J. Huo and X. F. Chen, Opt. Express **20**, 13419–13424 (2012).
[21] F. Xu, J. Liao, X. J. Zhang, J. L. He, H. T. Wang, and N. B. Ming, Phys. Rev. A **68**, 033808 (2003).